Astron. Astrophys. 324, 137–154 (1997)

ASTRONOMY
AND
ASTROPHYSICS

Eclipsing binaries with candidate CP stars

I. Parameters of the systems HD 143654, HD 184035 and HD 185257⋆,⋆⋆

P. North, M. Studer, and M. Künzli

Institut d'Astronomie de l'Université de Lausanne, CH-1290 Chavannes-des-Bois, Switzerland

Received 6 November 1996 / Accepted 3 February 1997

Abstract. Lightcurves of three eclipsing binaries (HD 143654 = TV Nor, HD 184035 = HR 7422 and HD 185257 = HR 7464) in seven colours are analyzed and their photometric elements are given. Published radial velocities of two of them allow some constraints to be put on the masses of the components, while new radial velocities allow us to estimate the mass and absolute radius of each component of the system TV Nor. There seems to be no Ap star in this system, in spite of its EuCrSr classification in the Michigan catalogue. The position of each component of TV Nor in the HR diagram is in excellent agreement with stellar evolution models having $Z = 0.020$ and an age $t = 2.51 \times 10^8$ years.

There is an Am star in the system HD 185257, but no CP star in the system HD 184035 in spite of its sharp lines. The physical parameters of these two binaries could be determined, but less accurately and in a less fundamental way than those of TV Nor. They match theoretical isochrones and evolutionary tracks in a satisfactory way for HD 185257, but the measured mass function of HD 184035 seems slightly too small compared with the expected theoretical masses.

More data, both photometric and spectroscopic, would be useful, especially for the last two systems.

Key words: stars: binaries: eclipsing – stars: binaries: spectroscopic – stars: chemically peculiar – stars: early-type – stars: fundamental parameters – stars: individual: HD 143654, HD 184035, HD 185257

1. Introduction

Binarity is a very important parameter to consider when dealing with any kind of chemically peculiar stars (hereafter CP stars). It is well known that there is a strong deficiency of close binaries among CP2 (magnetic Ap) stars (Gerbaldi et al. 1985, North 1994). Even among CP1 (Am) stars, whose large majority belong to binary systems, there is a clear deficit of very short orbital periods compared with systems hosting normal stars. Therefore, the number of confirmed CP2 stars in eclipsing systems is vanishingly small, while such systems would be of great interest: very few Ap stars have fundamentally determined parameters; furthermore, if the Ap component turns out to be a spectroscopic variable, its detailed observation when it enters into eclipse may provide strong constraints on the distribution of the abundance anomalies on its surface, complementing the more usual Doppler imaging technique (Vincent et al. 1993).

As yet, there are only a handful of Ap stars in eclipsing binaries, and some of them may well have a spurious classification (North & Burnet 1994, North & Richard 1995). The best studied case is that of a CP3 (HgMn) star, AR Aur (Nordström & Johansen 1994; Johansen & Nordström 1995) - which is non-magnetic - followed by AO Vel, which is the unique Si-type eclipsing binary known (Clausen et al. 1995). The classification of the latter remains to be confirmed, however, even though its lightcurve provides clear evidence for an intrinsic and strictly periodic variation of at least one component. A close examination of other cases is then useful, and is beginning with this work. Am stars are more frequently found in eclipsing systems, and at least ten of them have very precisely determined parameters (Andersen 1991), but Andersen and his coworkers avoided any kind of Ap star in their monumental work on detached systems.

HD 143654 (TV Nor), HD 184035 (HR 7422) and HD 185257 (HR 7464) are three detached eclipsing binaries, which have been observed in the seven-colours Geneva photometric system but have not yet been studied in detail.

The first one, TV Nor, was studied in a preliminary way by North & Burnet (1994), who gave an estimate of its total mass from a spectrum taken at a quadrature, but did not interpret its lightcurves. Here we determine for the first time the solution of the lightcurves, and additional spectroscopic data allow us to propose a complete solution of the system. This binary had been brought to the attention of observers by Renson (1990) as

Send offprint requests to: P. North

⋆ Based on observations collected at the European Southern Observatory, La Silla, Chile

⋆⋆ Tables 1, 2 and 3 are available only in electronic form at the CDS via anonymous ftp 130.79.128.5

one of the very few eclipsing binaries with an Ap classification. This was the main motivation for observing it.

The two other systems were discovered by Waelkens & Rufener (1983), who just gave their orbital period and V lightcurve. HD 184035 was already known as an SB1 spectroscopic binary and has published radial velocity curve and orbital elements (Buscombe & Morris 1961); however, the mass ratio cannot be directly obtained since the lines of the secondary component have not been observed. Gaspani (1984) proposed a solution of the Geneva V lightcurve of HD 184035, while Giuricin et al. (1984) did the same for HD 185257. Levato (1975) measured $V \sin i$ = 60 km s^{-1} for the primary of HD 184035. On the basis of Geneva photometry alone, Waelkens & Rufener (1983) could assign an A5m *photometric* spectral type to the primary of HD 185257 (Hauck & Curchod 1980 had also suspected this star to be an Am from its Geneva indices). Their determination was nicely confirmed by Houk (1982), who gives the spectral type A1mA6-F0 to this binary, the quality of the classification spectrum being 1, i.e. the best; here A1 is the type derived from the calcium lines, A6 is derived from the hydrogen lines and therefore should represent best the real effective temperature of the star, and F0 is the type derived from the metallic lines. Therefore the photometric type agrees with the spectroscopic one within one subclass. In fact, the Am peculiarity of HD 185257 was already known from the work of Andersen & Nordström (1977) and even from earlier litterature, since these authors quote an A2m type.

In this sample of three eclipsing binaries, two systems seem *a priori* to contain one chemically peculiar star, which enhances their astrophysical interest. We shall question below, however, the Ap nature of TV Nor. The third system has been mentioned as showing "unusually sharp lines for an A-type star" by Buscombe & Morris (1961), which may be considered as implicitly designating the primary as a CP star, if the conclusions of Abt & Morrell (1995) hold true.

Here we analyze all seven lightcurves of each system and propose in addition an orbital solution for the primary of HD 185257, which has 9 published radial velocities (Catchpole et al. 1961, Nordström & Andersen 1985).

2. Observations and reductions

All photometric observations have been done at the European Southern Observatory, La Silla, Chile, with the Swiss telescope equipped with the double-beam "P7" photometer (Burnet & Rufener 1979). The Swiss telescope was a 0.4m one before April 1980, and a 0.7m one after. As is usually the case with the Swiss telescope, a large variety of observers contributed to the lightcurves, so it is impossible to list them all. C. Waelkens made numerous observations of HD 184035 and HD 185257 in 1981. M. Burnet and P. North made most observations of HD 143654; the first three, routine measurements were made as early as 1982, 1983 and 1984 respectively, and five additional measurements were made in April 1989 by the regretted Dr. Zdenek Kviz. Systematic monitoring began especially in June 1990, stimulated by Renson's IBVS note, and continued each following season until July 1994; E. Paunzen (Vienna) participated in the measurements made in July 1994.

The visual magnitude and colour indices have been reduced in the standard way, i.e. as all-sky measurements, although in the case of TV Nor, the nearby standard star HD 141318A (HR 5873, type B2II, V=5.759) has generally been observed just before or after. They are listed in Tables 1 to 3 (available in electronic form only) for HD 143654, HD 184035 and HD 185257 respectively.

Since there is as yet no published radial velocity of the TV Nor system, PN made five spectroscopic observations of it with the CAT 1.4m telescope and CES spectrograph at ESO, La Silla, Chile, to obtain accurate V_r data and, ultimately, the individual masses of the components. An observation with the Coravel scanner (Baranne et al., 1979) had been kindly attempted by Dr. Jean-Claude Mermilliod at the 1.54m Danish telescope at ESO, but no autocorrelation peak could be seen; the meaning of this negative result is discussed in the next section.

The first spectrum has been taken in May 1994 in a 61 Å wavelength range centered on 6562 Å, i.e. on the H_α line. We used the Long Camera in the Red Path. The detector was a Ford Aerospace CCD with 2048 pixels measuring 15 × 15μm (designation FA2048 L, ESO CCD #30). This chip is frontside illuminated and UV coated; it does not suffer any severe fringes, even in the red. The resolving power was R=60000, which implies a 0.11 Å resolution, a reciprocal dispersion of 0.03 Å per pixel and a sampling of 3.65 pixels per resolution element. In this spectral region, many telluric lines are present, essentially due to the H_2O molecule. Therefore, the spectra have to be corrected for them. To this purpose, we observed the bright, rapidly rotating ($V \sin i$ = 361 km s^{-1}) A0V star HR 5511 at almost the same airmass (1.22) as that of TV Nor (1.25). The stability of the spectrograph has been quite good during this night: the shift between the thorium lines measured before the night and those measured just after TV Nor was 0.23 pixels, i.e. about 7 mÅ or 0.3 km s^{-1}.

The other spectra have been taken in July 1996, in a 68 Å wavelength range centered on 5890 Å, i.e. on the Na I D lines. Again the Long Camera and Red Path were used, but the detector was the ESO CCD #38, a LORAL/LESSER, thinned and backside illuminated chip with 2688 × 512 pixels measuring 15 × 15μm. The quantum efficiency of this CCD is impressive: it is close to 90% at the wavelength we used. Here too, numerous telluric lines are present and must be corrected for. The rapidly rotating ($V \sin i$ = 260 : km s^{-1}) B8Vn star HR 6500 was observed for that reason.

The reductions of the spectra have been made using the IHAP software, in a rather standard way, including the rebinning to a wavelength step of 0.01 Å.

The journal of the spectroscopic observations is given in Table 4, together with the radial velocities obtained for each component of TV Nor.

Table 4. Journal of the spectroscopic observations of TV Nor. The epochs are barycentric julian dates corresponding to the middle of the exposure.

TV Nor comp.	HJD −2400000	t_{exp} [s]	phase	$V_r \pm \sigma(V_r)$ [km/s]		λ_c [Å]
A	49489.608	2700	0.2525	-77.0	1.2	6562
B				84.5	1.2	
A	50279.686	1800	0.9367	23.52	0.5	5890
B				-39.18	0.5	
A	50280.692	3600	0.0548	-29.52	0.5	5890
B				25.27	0.5	
A	50281.674	2400	0.1700	-68.03	0.5	5890
B				73.58	0.5	
A	50282.575	3600	0.2757	-75.72	0.5	5890
B				82.98	0.5	

3. Results

3.1. HD 143654 (TV Nor)

This star was long known as an eclipsing binary (Kruytbosch 1930) and its orbital period has been accurately determined by Hertzsprung (1937). It has been classified Ap EuCrSr by Houk (1978) so that one should expect, *a priori*, an out-of-eclipse, periodic variability of the α CVn type linked with the Ap nature of e.g. the primary component. The amplitude of this variability may also be expected to be small (a few hundredths of a magnitude at most), because of the dilution of the Ap component's light by the light of the other component.

3.1.1. Photometry

Preliminary results have been published by North (1994) and North & Burnet (1994), showing that the system is well detached and that no significant out-of-eclipse variation can be seen either in the V magnitude or in the colour-indices, contrary to what the Ap classification would suggest. Fig. 1 shows the updated lightcurve for the V magnitude as well as for the colour indices $[U-B]$ and $[B-V]$, according to the ephemeris

$$HJD(MinI) = 2448745.8321 + 8.524391E \pm 0.0002 \pm 0.000008 \quad (1)$$

obtained from the combination of our data and the epochs of primary minima published by Hertzsprung (1937). The period obtained by that author, 8.524406 days, was very close to ours. There are 161 measurements in each of the 7 passbands of the Geneva system. This is a relatively small number, but the minima are well defined. The whole Min I has been observed on two different nights, and its descending branch on a third night. Different parts of Min II were observed during six nights, while the out-of-eclipse magnitudes have been gathered on about 40 different nights. One immediately sees that the two components do not have the same effective temperature, since the $[B-V]$ index varies in opposite directions in the primary and secondary minima. On the other hand, $[U-B]$ does not vary, indicating that this index is the same for both components, so that they must have spectral types either between B9 and A5 or between F0 and G0.

Another interesting feature of the V lightcurve is the flat bottom of the secondary minimum, indicating a total eclipse (occultation). This is consistent with the hotter star being also the larger (and the brighter): Minimum II is an occultation while Minimum I is a transit. The bottom of Minimum I is not flat because of the limb-darkening of the primary; on the other hand the system appears bluer at Min. II and redder at Min. I. All this indicates two main-sequence stars having slightly different masses.

Finally, the luminosity of the system remains perfectly stable between the eclipses, contrary to the slight, possibly double-waved modulation one would expect from the presence of an Ap component: since the photometric variations of Ap stars are due to the inhomogeneous distribution of the abundances on the surface of the star, their period is the same as the spin period, and also the same as the orbital period if synchronization is assumed. Therefore, the Ap nature of one of the components (or of both) appears doubtful according to this purely photometric evidence.

Interstellar reddening and effective temperatures of the components: The total eclipse allows us to determine the colour indices of each component with an excellent accuracy. However, the colours are affected by interstellar reddening, since the star lies on the galactic plane, only 29 degrees from the Galactic Center ($l2 = 331^o, b2 = +1^o$) where the colour excess $E(B-V)$ reaches about $0.2-0.4\ mag\ kpc^{-1}$ (Lucke 1978). Table 5 lists the magnitude and colours of the whole system and of each component, obtained respectively from the average of the out-of-eclipse data and from the average of the six measurements made in the bottom of the secondary minimum. Fig. 2a-d shows the location of each component of TV Nor in four photometric diagrams: $[U-B2]/[B2-G]$, $d/[B2-V1]$, $[U-B2]/[B2-V1]$ and $[U-B1]/[B2-G]$. The unpublished ZAMS from Burki et al. (1993) is shown, together with the sequence of the intrinsic colours of the MK types for the luminosity classes V and III (Hauck 1994). In the $d/[B2-V1]$ diagram we have added the reference Hyades sequence of Hauck (1973). The points are represented with a reddening line corresponding to $E(B2-V1) = 0.15$ (the colour-excess ratios have been taken from Cramer 1994). One sees that this amount of reddening would bring both components exactly to the empirical ZAMS on Fig. 2d, but slightly "above" it (imagining the HR diagram) on the other diagrams. The cause of this discrepancy is not very clear. It might be linked with some anomalous reddening, which does exist in the Upper Scorpius and ρ Ophiuci regions (Whittet 1974, Wu et al. 1980, North 1984), some 25° from TV Nor. We adopt here $E(B2-V1) = 0.15$.

With this colour excess, we obtain $T_{eff} = 9123 \pm 135$ K for the primary and $T_{eff} = 7788 \pm 73$ K for the secondary component, using the calibration of Künzli et al. (1997). The surface gravities obtained are $\log g_1 = 4.13 \pm 0.03$ and $\log g_2 = 4.40 \pm 0.07$ respectively (where the uncertainties result only from the propagation of typical photometric errors, disregard-

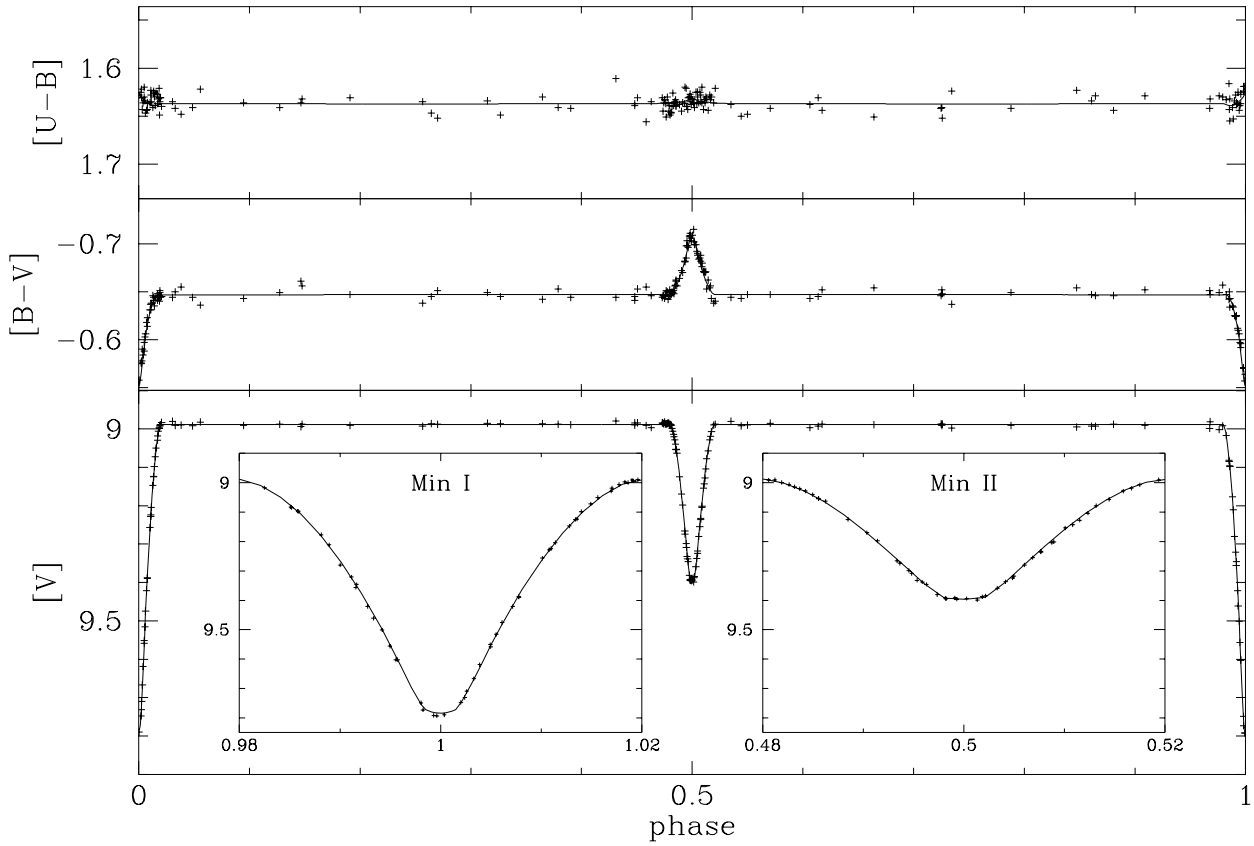

Fig. 1. Lightcurves of TV Nor in the V magnitude and in the $[U-B]$ and $[B-V]$ indices. The fitted lightcurves are those computed by the EBOP code for the adopted parameters of Table 6.

Table 5. Magnitude and colours of each component of the TV Nor system. The peculiarity parameter $\Delta(V1-G)_o$ and the the metallicity parameter Δm_2 are corrected for the effect of interstellar reddening. The combined colours of the whole system are given too.

object	m_V	$[U-B]$	$[V-B]$	$[B1-B]$	$[B2-B]$	$[V1-B]$	$[G-B]$	$\Delta(V1-G)$	$\Delta(V1-G)_o$	Δm_2
primary	9.395	1.633	0.709	0.936	1.446	1.419	1.838	-0.004	0.002	0.002
secondary	10.255	1.649	0.497	0.984	1.376	1.219	1.598	-0.013	-0.007	0.000
whole syst.	8.989	1.637	0.647	0.949	1.426	1.361	1.767			

ing any systematic error), but these values are much less reliable than the fundamental ones determined below.

In the light of the $T_{\rm eff}$ obtained above, it is interesting to recall that no autocorrelation dip could be seen with the CORAVEL scanner. This is completely normal as far as *normal* stars are considered, since the CORAVEL mask is valid for cool stars and cannot yield a significant dip for spectral types earlier than about F0. However, Ap stars *do* yield a dip, thanks to their large overabundance of some elements, like Cr, and to their slow rotational velocity: a sharp dip is observed even for Ap stars as hot as 8600 K (Wade et al. 1996). Therefore, the lack of any dip is a strong argument against the Ap nature of whatever component of TV Nor.

From the colours of the individual components (Table 5), the photometric parameter of peculiarity $\Delta(V1-G)$ can be computed from the formula:

$$\Delta(V1-G) = (V1-G) - 0.289(B2-G) + 0.302 \qquad (2)$$

(see e.g. Hauck 1974). The result is given in Table 5: in both cases, $\Delta(V1-G)$ is negative, which is quite typical of normal stars. Ap stars have at least a positive value, and most have $\Delta(V1-G) \geq 0.010$, although it is not always the case of the cooler ones, i.e. those of the SrCrEu type. The $\Delta(V1-G)$ parameter is slightly sensitive to reddening: it *decreases* with reddening (Hauck & North 1982) so that the values computed from Eq. 2 must be slightly increased. For $E(B2-V1) = 0.15$, the correction is 0.006 magnitudes. Hence the secondary is completely normal (since normal stars have $\Delta(V1-G) = -0.005$ on average) while the primary might have a very marginal peculiarity, though it is hardly significant.

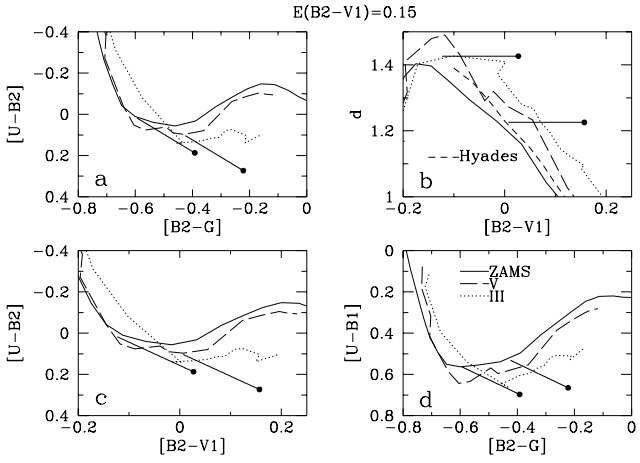

Fig. 2a–d. Position of the components of TV Nor in various photometric diagrams. In each diagram, the primary is the leftmost dot. The heavy segments protruding from the points are reddening lines corresponding to $E(B2-V1) = 0.15$. The continuous line is the ZAMS from Burki et al. (1993), the long-dashed and dotted lines represent the average colours of consecutive spectral types for the luminosity class V and III respectively (from Hauck 1994); the short-dashed line in **b** is the Hyades' reference sequence from Hauck (1973).

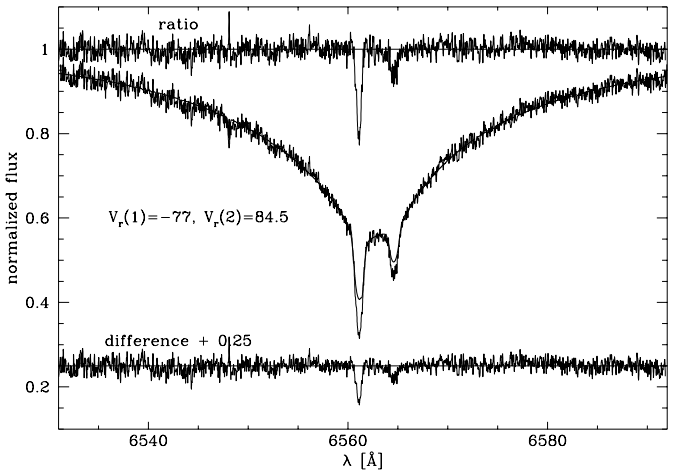

Fig. 3. H_α observation of the TV Nor system near the quadrature (phase 0.2525). The sum of synthetic spectra with $T_{\rm eff}$ = 9125, 7790 K and $\log g$ = 4.21, 4.27 dex is shown (heavy line). The ratio of the observed and synthetic spectrum is shown at the top of the figure, while the difference (increased by 0.25 for clarity) is shown at the bottom of the figure.

The m_2 photometric parameter, defined by Hauck (1973), is useful to test whether one or both components may be considered as Am stars:

$$m_2 = (B1 - B2) - 0.457(B2 - V1) \quad (3)$$

The difference Δm_2 between m_2 and a reference value for the same $(B2 - V1)$ index is proportional to the metallicity of the stars (Hauck 1973, Hauck et al. 1991). Table 5 gives the Δm_2 values, and we see once again that they are typical of normal stars. The test is not entirely conclusive since many Am stars do have a small Δm_2, but at least can we be sure that no component (especially the secondary, whose effective temperature is more typical of Am stars) of TV Nor is an extreme Am star. The definitive answer can only be given by a spectrum showing calcium lines, since the Am peculiarity is defined by the deficiency of this element.

Determination of the photometric parameters: The lightcurves have been interpreted using the 16th version of the relatively simple code EBOP, which was kindly transmitted to us by Dr. Paul Etzel (1989) through the regretted Dr. Zdenek Kviz. The use of this code is completely justified by the lack of any significant proximity effect, betrayed by the flatness of the curve between the eclipses. PN had modified the EBOP16 code to make it display the observed and fitted lightcurve, and so that the parameters as well as their status (fixed or variable) can be modified interactively. It is this modified code that was used to obtain the solution, by first converging the inclination, the secondary's surface brightness, the magnitude at the quadrature and the phase correction. Then the primary's radius was "freed", together with the ratio of radii *k*, and finally the quantities $e\,cos\omega$ and $e\,sin\omega$. We even tried to determine the limb-darkening, but the results are not very reliable because of the relatively small number of data we have. Indeed, numerical experiments have been made with ten simulated lightcurves obtained by adding random, gaussian noise to a theoretical V curve containing 161 points at all observed phases, plus 56 points regularly spaced in phase (with a 0.002 step) in each minimum: both limb-darkening coefficients were then fitted, together with all other parameters of Table 6, and the mean as well as the external rms scatter of the fitted values were computed. It appears that, with these 273 pseudo-observations (whose average residual scatter, 0.0038, is slightly better than in the real case), the external scatter of u_1 is 42% higher than the formal sigma given by the code, while the external scatter of u_2 agrees quite well (within 7%) with the formal sigma. The underestimate of the error on u_1 can be explained by the strong correlation between r_1/a and u_1. The means of the 10 fitted values fall within 0.02 of the original ones (u_1 = 0.428 and u_2 = 0.456 instead of 0.453 and 0.472 respectively), which fulfills the statistical expectation, but a single fit may easily be off by 0.1. A good determination of the limb-darkening coefficients would need at least 500 data points per minimum, especially for the Min I where only 76% of the primary's light is occulted.

We always assumed no third light, and the gravity darkening coefficients were set to 1. We left the code compute itself the reflection coefficients, which in any case are not really relevant. The mass ratio was arbitrarily set to 1, since it has no influence in practice here.

Table 6 lists the photometric parameters obtained separately for each magnitude of the Geneva system, and for two cases: first, the linear limb-darkening coefficients were not adjusted, but were fixed to the values given for the $T_{\rm eff}$ determined above

and for the fundamental $\log g$ (see below) in the tables of Wade & Rucinski (1985); second, the limb-darkening coefficients were fitted. In that case, if $e\cos\omega$ and $e\sin\omega$ were fitted at the same time, the code tended to lower the inclination until no total eclipse occurs; but this is clearly a numerical problem of convergence, because the scatter of the residuals were larger than with a total eclipse. An attempt to fit $e\cos\omega$ and $e\sin\omega$ to the $[B]$ data resulted in $e\cos\omega = -0.00005 \pm 0.00007$ and $e\sin\omega = 0.0026 \pm 0.0059$, so that these quantities are not significantly different from zero. The adopted geometric parameters are listed in the last column. The errors listed in Table 6 are the formal ones given by EBOP. However they seem quite realistic, at least for this particular system and in the case where the limb-darkening coefficients are kept fixed: to verify that, a set of ten artificial lightcurves were computed by adding random errors to the theoretical $[V]$ curve (sampled at the observed phases), and EBOP was converged on each. The external rms scatter was then computed for each of the fitted parameters (i, r_1/a, k and J_2/J_1) and found to be consistent (within 25% at most) with the formal, internal error given by the code. The external error is even smaller than the formal one for all parameters but i. The average value of the fitted coefficients coincide with those fitted to the observed curve within half a sigma. Naturally, an additional, systematic error exists, which follows from possibly wrong limb-darkening coefficients adopted. However such an error is likely to be small, as a comparison between both parts of Table 6 shows.

When the same simulation is carried out relaxing u_1 and u_2 as variable ($SFACT$ and $\Delta\theta$ are also considered unknown in all these simulations), the situation worsens: the external scatter becomes larger than the formal one (by up to 50-100%), especially for i, u_1 and $J2/J1$, and the average value may be off by two sigmas. Keeping u_1 and u_2 fixed but changing the value of u_1 by ± 0.1 implies a change of r_1 and r_2 of no more than 0.8% and 0.1% respectively, while changing u_2 by ± 0.1 (with u_1 at its hopefully right value) changes r_1 and r_2 by 0.01 and 0.08% respectively, which is negligible (but J_2/J_1 changes by more than 3%).

We also used Wood's (1972) WINK code (version 10, 1982) to check the results obtained with EBOP16, and the results are presented in Table 7. The ratio of the central surface brightnesses is replaced there by the effective temperature of the secondary, the one of the primary being given by the user. We have updated the theoretical fluxes used by WINK by replacing the original ones by those of Kurucz (1995). The limb-darkening coefficients were considered constant (at the value interpolated in the tables of Wade & Rucinski 1985); otherwise, convergence problems arise. We assumed $T_{\rm eff}(1) = 9125$ K for the primary. The results are encouraging, in that the geometric parameters are the same as those obtained from EBOP16, within the errors. The effective temperature of the secondary is in fair agreement with that obtained through the photometric calibration of the colour indices, except for the $[U]$ data.

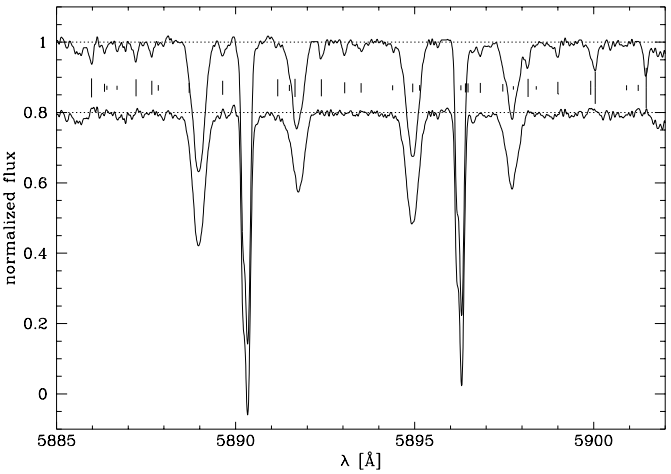

Fig. 4. Spectrum of TV Nor taken on HJD 50281.674, showing the Na I doublet for each component, as well as for the interstellar medium on the line of sight. The upper spectrum is the raw one including the telluric lines; the lower spectrum is corrected for the telluric lines. The vertical bars between both spectra indicate the wavelengths and equivalent widths (proportional to the height of the bar) of the telluric lines (Moore et al. 1966) with $W_\lambda > 3$ mÅ. The spectra are not corrected for the Earth's velocity.

3.1.2. Spectroscopy

Five spectra have been taken to define the radial-velocity curve and look for possible emission of circumstellar gas. One was taken in the H_α region, the others in the region of the Na I D lines.

The H_α spectrum: The observation made in H_α in May 1994 is shown in Fig. 3, together with a superposition of two synthetic spectra computed with the help of Hubeny's SYNSPEC code and Kurucz (1995) atmosphere models with $T_{\rm eff}$ = 9125, 7790 K and $\log g$ = 4.21, 4.27 dex. The flux ratio at H_α was set to 2.079; both synthetic spectra have $[M/H] = 0.0$, a microturbulence velocity $\xi_t = 2.5$ km s^{-1} and no rotational velocity; they were convoluted by a gaussian with $FWHM = 0.11$ Å, representing the instrumental profile. The Balmer line profiles were computed with the VCS theory (Vidal et al. 1973). We show here the optimum fit, which allowed to determine the radial velocities of the components at that phase. Indeed, it is not sufficient to fit separately e.g. a gaussian to each line core for a good V_r determination, since the slope of the line wing on which it is superposed is large and will induce a systematic shift; this is why the Balmer lines are generally avoided in V_r determination of SB2 binaries. Once normalized to the continuum (which was defined iteratively with the synthetic spectrum as a guide), the stellar spectrum was divided by the spectrum of the telluric lines. The latter was obtained by normalizing the observed spectrum of the rapidly rotating A0V star HR 5511 to 1, the whole stellar spectrum being considered as the continuum. Since the airmasses of TV Nor and HR 5511 were very close,

Table 6. EBOP16 solution of the 7 lightcurves of the TV Nor system. In the first case the limb-darkening coefficients have been kept fixed; in the second case they were determined. $e\cos\omega$ and $e\sin\omega$ were set to zero in both cases. Listed in the last column are the adopted geometric parameters.

parameter	$[U]$	$[B]$	$[V]$	$B1$	$B2$	$V1$	G	Adopted
i (degrees)	89.64	89.628	89.748	89.76	89.95	89.738	89.79	89.708
	±0.11	±0.068	±0.073	±0.12	±0.25	±0.092	±0.14	±0.070
r_1/a	0.06725	0.06790	0.06774	0.06760	0.06747	0.06750	0.06808	0.06768
	±0.00033	±0.00022	±0.00017	±0.00024	±0.00026	±0.00023	±0.00028	±0.00017
k	0.8424	0.8416	0.8430	0.8424	0.8416	0.8440	0.8389	0.8422
	±0.0058	±0.0039	±0.0028	±0.0042	±0.0045	±0.0038	±0.0043	±0.0028
r_2/a	0.05665	0.05715	0.05710	0.05695	0.05678	0.05697	0.05711	0.05703
	±0.00048	±0.00032	±0.00024	±0.00035	±0.00037	±0.00032	±0.00038	±0.00024
u_1	0.497	0.578	0.453	0.558	0.551	0.451	0.423	
u_2	0.620	0.558	0.472	0.573	0.541	0.480	0.451	
J_2/J_1	0.5494	0.5280	0.6461	0.5099	0.5641	0.6429	0.6727	
	±0.0042	±0.0025	±0.0022	±0.0029	±0.0033	±0.0030	±0.0037	
σ_{res} (mag)	0.0080	0.0050	0.0042	0.0059	0.0064	0.0055	0.0066	
i (degrees)	89.47	89.483	89.532	89.52	89.56	89.495	89.38	
	±0.14	±0.091	±0.070	±0.11	±0.13	±0.093	±0.12	
r_1/a	0.06800	0.06818	0.06842	0.06831	0.06810	0.06856	0.06977	
	±0.00070	±0.00042	±0.00031	±0.00051	±0.00052	±0.00043	±0.00050	
k	0.8372	0.8410	0.8375	0.8381	0.8386	0.8346	0.8256	
	±0.0086	±0.0053	±0.0040	±0.0063	±0.0065	±0.0056	±0.0075	
r_2/a	0.05692	0.05734	0.05731	0.05725	0.05711	0.05722	0.05760	
	±0.00083	±0.00051	±0.00038	±0.00061	±0.00062	±0.00053	±0.00067	
u_1	0.63	0.634	0.583	0.680	0.668	0.646	0.730	
	±0.10	±0.060	±0.046	±0.068	±0.072	±0.060	±0.071	
u_2	0.71	0.785	0.638	0.72	0.77	0.545	0.58	
	±0.15	±0.086	±0.068	±0.11	±0.11	±0.099	±0.12	
J_2/J_1	0.547	0.566	0.661	0.520	0.593	0.621	0.642	
	±0.034	±0.021	±0.019	±0.024	±0.027	±0.024	±0.028	
σ_{res} (mag)	0.0080	0.0049	0.0040	0.0058	0.0063	0.0054	0.0063	

such a simple procedure sufficed in removing the telluric lines within the S/N ratio of the stellar spectrum.

Because of the short wavelength range of the observed spectrum, hence the impossibility to define a purely empirical continuum, the effective temperatures can not be constrained efficiently. Interestingly, the very centers of the lines are not well reproduced by the synthetic spectra: the observed profiles are sharper and deeper than the computed ones, while the contrary would be expected, especially as the stars probably rotate in synchronism with the orbital period, i.e. at about 10 km s^{-1}. The difference might be due to an unsatisfactory modelling of the uppermost atmosphere layers in the Kurucz models and of the Balmer line cores in the VCS theory. On the other hand, this spectrum shows no obvious emission feature, so that no gas stream is present and the system is indeed well detached.

The Na i D lines and radial-velocity curve: The four spectra taken in 1996 were much better suited for V_r measurements, thanks to the flat continuum and the strength of the Na I D lines. However, many telluric lines are present, so that we averaged three spectra of the rapidly rotating B8Vn star HR 6500 after having normalized them in the appropriate way. Since they were taken at various airmasses, the spectra of the telluric lines had to be transformed through the formula:

$$s(corrected) = (s + a)/(1 + a) \quad (4)$$

to make the depths of the telluric lines equal in all three of them; here s is the flux and a is a constant which is positive when weaker lines are needed and negative in the opposite case (see also North et al. 1994). An average weighted by $(S/N)^2$ was taken of the telluric spectra, and the spectra of TV Nor were divided by the average spectrum previously transformed by formula 4. An example of the raw and corrected spectra of TV Nor is shown on Fig. 4. Not only are the stellar lines clearly visible for both components, but the interstellar Na I D lines are also very conspicuous. They offer a unique opportunity to check the stability of the wavelength scale.

The IS lines can be very well fitted by two gaussians each, so it seems there are two interstellar clouds along the line of sight. The barycentric radial velocity of each cloud is given in Table 8 together with the average parameters of the fitted gaussians. Based on the position of these lines, the stability of the wavelength scale is in any case better than 0.4 kms^{-1}. A gaussian was fitted to the Na I D lines of the stellar components and we obtained the radial velocities listed in Table 4. Having two lines

Table 7. WINK10 solution of the 7 lightcurves of the TV Nor system. the limb-darkening coefficients have been kept fixed, as well as e and ω. For the primary, $T_{\rm eff}(1)$ = 9125 K was assumed.

parameter	$[U]$	$[B]$	$[V]$	$B1$	$B2$	$V1$	G
i (degrees)	89.61	89.629	89.739	89.714	89.807	89.723	89.720
	±0.10	±0.062	±0.053	±0.077	±0.085	±0.067	±0.080
r_1/a	0.06710	0.06790	0.06767	0.06757	0.06744	0.06747	0.06807
	±0.00041	±0.00024	±0.00017	±0.00026	±0.00029	±0.00025	±0.00029
k	0.8472	0.8426	0.8450	0.8441	0.8425	0.8451	0.8397
	±0.0096	±0.0061	±0.0042	±0.0065	±0.0064	±0.0055	±0.0061
r_2/a	0.05685	0.05721	0.05718	0.05704	0.05682	0.05702	0.05716
	±0.00073	±0.00046	±0.00032	±0.00049	±0.00050	±0.00043	±0.00048
u_1	0.497	0.578	0.453	0.558	0.551	0.451	0.423
u_2	0.620	0.558	0.472	0.573	0.541	0.480	0.451
$T_{\rm eff\,2}$	7585	8007	7978	8000	8023	7998	7977
	±17	±7	±7	±8	±10	±10	±13
σ_{res} (mag)	0.0075	0.0047	0.0039	0.0055	0.0060	0.0051	0.0061

Table 8. Radial velocities of the two interstellar clouds lying in the line of sight of TV Nor. The equivalent widths and FWHM of the lines are also given.

Cloud #	V_r [km s^{-1}]	Na I λ [Å]	W$_\lambda$ [mÅ]	FWHM [mÅ]
1	-5.32	5889.950	57.6	122
	±0.16		±1.7	±5
		5895.924	45.7	112
			±0.4	±1
2	1.76	5889.950	152.4	169
	±0.14		±0.5	±4
		5895.924	125.2	154
			±0.8	±1

is useful to check the consistency of the radial velocities: the largest difference between the V_r derived from the two lines is 0.36 km s^{-1} for the primary and 0.60 km s^{-1} for the secondary. This is why we assumed an uncertainty of 0.5 km s^{-1} on the average radial velocities in Table 4.

We fitted the orbits on the 10 points of Table 4, assuming a null eccentricity and fixing the period and the epoch according to the photometric ephemeris. The fitted parameters are therefore only the systemic velocity and both amplitudes. Table 9 gives the results and Fig. 5 shows the radial-velocity curves. In spite of the very small number of points, the results are quite precise thanks to the excellent accuracy of the V_r measurements. The only weak point might be the assumption e = 0.0; however, if e is allowed to vary, it converges to the value e = 0.0035 ± 0.0023, which confirms the photometric solution pointing to a negligible eccentricity. The standard deviation of the residuals is 0.28 km s^{-1} only, confirming the high precision of the V_r determinations.

Physical properties of the TV Nor system: Synthetic spectra of both companions of TV Nor have been computed in the region of the Na I D lines and have been superposed, in the same way as for the H_α region (Fig. 6), to the last spectrum, taken close to the qadrature. We obtained a very good fit of both Na I lines of the secondary with a nearly solar composition ($\log\epsilon = -5.76$), $T_{\rm eff}$ = 7790K, $\log g$ = 4.27, a microturbulence velocity $\xi_{\rm t}$ = 2.5 km s^{-1} and a projected rotational velocity $v \sin i$ = 11.3 km s^{-1}. For the primary, the fit was less satisfactory: we had to increase the abundance to 1.5 × that of the secondary ($\log\epsilon = -5.59$), and chose $v \sin i$ = 13 km s^{-1}. For a few Fe I lines, the solar abundance ($\log\epsilon = -4.33$) seems appropriate, especially for Fe I λ5905.689 ($\log gf = -0.622$ according to Kurucz 1989, which agrees well with $\log gf = -0.73$ from Fuhr et al. 1988) and for the blend Fe I λ5914.114 + 5914.194 ($\log gf = -0.444$ and -0.059 from Kurucz 1989). It is difficult to judge whether the slight difference in the Na abundance between the primary and the secondary is real, since the lines are strongly saturated. We took the broadening parameters from the VALD database (Piskunov et al. 1995), and verified that the microturbulence has a negligible effect. Na can be overabundant in Am stars (see e.g. van't Veer-Menneret et al. 1985, Fig. 5), so that an overabundance of it in the primary's atmosphere would not be excluded as far as it is not representative of the global metallicity of the star; but apart this 0.18 dex difference between the binary's components in the Na abundance, the present data are compatible with a nearly solar metallicity.

The $v \sin i$ values are interesting to consider in relation with the orbital period. If there was a perfect synchronism between the spin and orbital period, then one should expect $v_1 \sin i$ = 10.9 km s^{-1} and $v_2 \sin i$ = 9.2 km s^{-1}. Therefore, there is marginal evidence that both components rotate about 20% faster than expected from synchronism. Spectra with higher resolution and better S/N ratio would be needed to settle this question definitely. The adopted physical parameters are listed in Table 10, where the uncertainties on the masses and radii have been arbitrarily doubled relative to the formal ones given in Tables 6 and 9; in this way, the errors given in Table 10 are probably safely realistic.

The location of both components on the HR diagram is shown in Fig. 7, together with the isochrone with $\log t$ = 8.4 (t in years) computed from the evolutionary tracks of Schaller

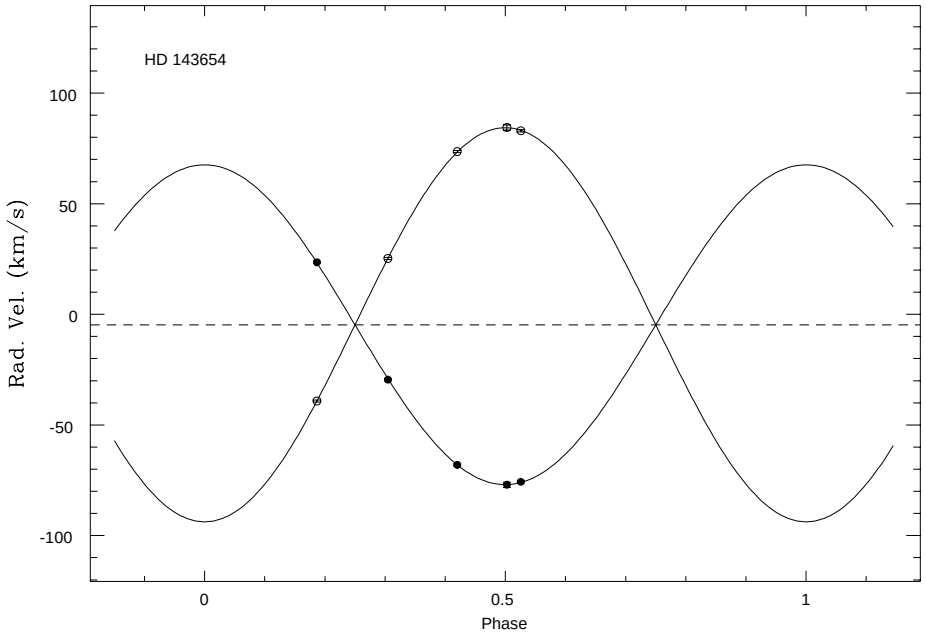

Fig. 5. Radial-velocity curves of the TV Nor system. The black dots represent the primary, the open dots the secondary. Notice that the error bars are smaller than than the size of the points. Here the zero phase corresponds to ω = 0.0 for the primary, but not to the primary eclipse, which would occur here at phase 0.25.

Table 9. Orbital elements of the TV Nor system. The second line gives the uncertainty on the fitted parameters. Zero uncertainty means that the corresponding parameter was considered as known and was kept constant.

Star name	P $days$	T$_\circ$ HJD -2450000	e	V$_\circ$ kms^{-1}	ω_1 $^\circ$	K$_{1,2}$ kms^{-1}	$\mathscr{M}_{1,2}\sin^3 i$	a$_{1,2}\sin i$ $10^6 km$	N	(O-C) kms^{-1}
HD 143654	8.524391	278.0941	0.000	-4.69	0.0	72.26	2.0525	8.470	5	0.28
	0.000000	0.0000	0.000	0.12	0.0	0.20	0.0112	0.023		
						89.07	1.6651	10.440	5	
						0.20	0.0095	0.020		

et al. (1992) which have Z = 0.02, i.e. a solar metallicity. The agreement is excellent, well within the error bars.

3.2. HD 184035 (HR 7422, V4089 Sgr)

This star has been classified A2V by Houk (1978). Although Gaspani (1984) already analyzed the published V lightcurve of this system, we give here a more complete discussion of both the photometry and the radial velocities.

3.2.1. Photometry

Waelkens & Rufener (1983) estimate the period at P = 4.62988 days. However, a period search based on Renson's (1978) method yields a slightly shorter period, and we adopt the ephemeris:

$$HJD(Min.I) = 2444833.83185 + 4.6283E \quad (5)$$
$$\pm 0.00080 \pm 0.0024$$

There are only 79 photometric measurements in each of the seven passbands, but they are well concentrated on both minima and there are enough data at other phases to define the out-of-eclipse variation. The $[U-B]$, $[B-V]$ and V lightcurves are displayed in Fig. 8. The depth of the minima is small, 0.2 mag only, but as with TV Nor, the secondary minimum (whose bottom is flat) is a total eclipse (occultation) while the primary minimum is a transit, as noticed by Gaspani (1984). There is a slight but significant colour change in the minima, showing that the stars have different effective temperatures. Between the minima, there is a slight variability typical of the components' distorsion: although the system is detached, there are significant tides.

Effective temperatures of the components: The total eclipse allows us to determine the colour indices of each component, in the same way as for TV Nor. Table 11 lists the magnitude and colours of the whole system and of each component. Here the situation is much less straightforward than with TV Nor, because the primary is distorted by tides: the average of the ten measurements made in the bottom of the secondary minimum gives its colours when it is viewed along the system's axis, i.e. when it is redder. In order to obtain the secondary's colours, one has to subtract this contribution of the primary from the brightness of the whole system *considered at the same phase*, i.e. at the secondary minimum. In practice, this implies an interpolation of the out-of-eclipse variation due to the elongated primary, which

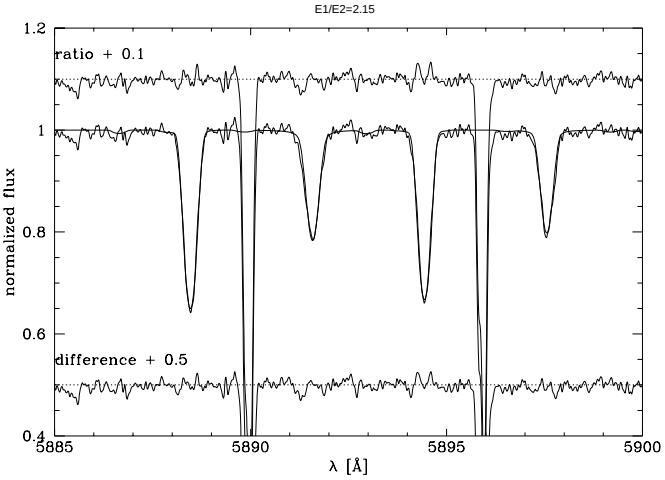

Fig. 6. Fit of the Na I D lines by synthetic spectra (see text). The heavy line is the synthetic spectrum, the thin line is the oberved one. The upper curve is the ratio of the observed and synthetic spectra (shifted by 0.1 for clarity) and the lower curve is the difference between them (shifted by 0.5). Here the spectrum, taken at HJD 50282.575, is in the barycentric reference frame.

Table 10. Physical parameters of the components of TV Nor. The errors on the masses and radii have been doubled (with regard to those in Tables 6 and 9) in order to make them more realistic.

	Primary	Secondary
$M/M_\odot$	2.053 ± 0.022	1.665 ± 0.018
$R/R_\odot$	1.839 ± 0.012	1.550 ± 0.014
$\log g$ [cgs]	4.221 ± 0.010	4.278 ± 0.012
$v \sin i$ [km s^{-1}]	13 ± 1	11.3 ± 1.0
$\log T_{\rm eff}$ [K]	3.960 ± 0.007	3.892 ± 0.006
$\log L/L_\odot$	1.325 ± 0.034	0.902 ± 0.035
M_{bol}	1.44 ± 0.09	2.50 ± 0.09
$B.C.$	-0.22	-0.12
M_v	1.66 ± 0.09	2.62 ± 0.09
$E(B2-V1)$	0.150 ± 0.015	
A_V	0.57 ± 0.06	
Distance [pc]	265 ± 14	

is relatively safe (the variation has the form $\cos(2\omega t+\phi)$). Since the ratio of radii is 0.406 (see below), the tidal effects should be much larger for the primary than for the secondary, so the latter may be rather safely be considered as spherical. This means that its colour do not depend on the orbital phase and that those computed for phase 0.5 are representative.

On the other hand, it is more delicate to obtain the colours which would be representative of the primary, i.e. corresponding to a similar, but spherical star. We give here the colours of the primary obtained at both phases 0.5 and 0.25, assuming that the colours of the secondary do not depend on the orbital phase. The colours vary only very slightly from ϕ = 0.5 to ϕ = 0.25. Fig. 9 shows the position of both components on the $d/B2-V1$ photometric diagram, with an assumed colour excess $E(B2-V1)$ = 0.02 which is probably an upper limit. One

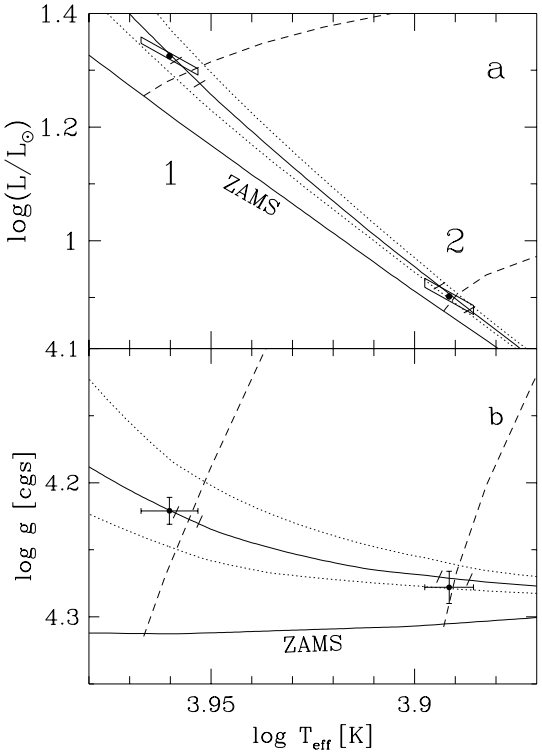

Fig. 7. a HR diagram of the TV Nor system. The solid lines are the theoretical ZAMS and the isochrone at $\log t$ = 8.4 (t in years) from Schaller et al. (1992). The dotted lines are the isochrones at $\log t$ = 8.3 and 8.5. The observed location of the components is indicated by the black dots and error boxes. The dashes crossing the isochrone indicate the uncertainties on the estimated masses, for which the evolutionary tracks are represented as broken lines. The errors are the amplified ones of Table 10. **b** Same as **a**, but for the surface gravity instead of luminosity on the y-axis. This diagram is more directly related with the observed fundamental quantities. The isochrones shown correspond to the metallicity Z = 0.020.

immediately sees that the primary is evolved. Using the recent calibration by Künzli et al. (1997) and adopting average colours for the primary, one obtains the physical parameters displayed in Table 12.

The values of the $\Delta(V1-G)$ and Δm_2 parameters are typical of normal stars, so there is no photometric evidence that either component be an Ap or an Am star.

Determination of the photometric parameters: We used both EBOP and WINK codes to solve each of the seven lightcurves, as for TV Nor. Table 13 shows the WINK results as well as the adopted parameters. Since the tidal distorsion is not negligible for the primary, the results of the WINK code should be preferred, although they agree with those of EBOP code within one sigma. A good fit to the observed curve could only be achieved by imposing the reflection coefficients w_1, w_2 to be zero in the WINK code. We tried to fit the linear limb-darkening coefficients simultaneously with the geometrical quantities, but without success: there are not enough data to constrain them

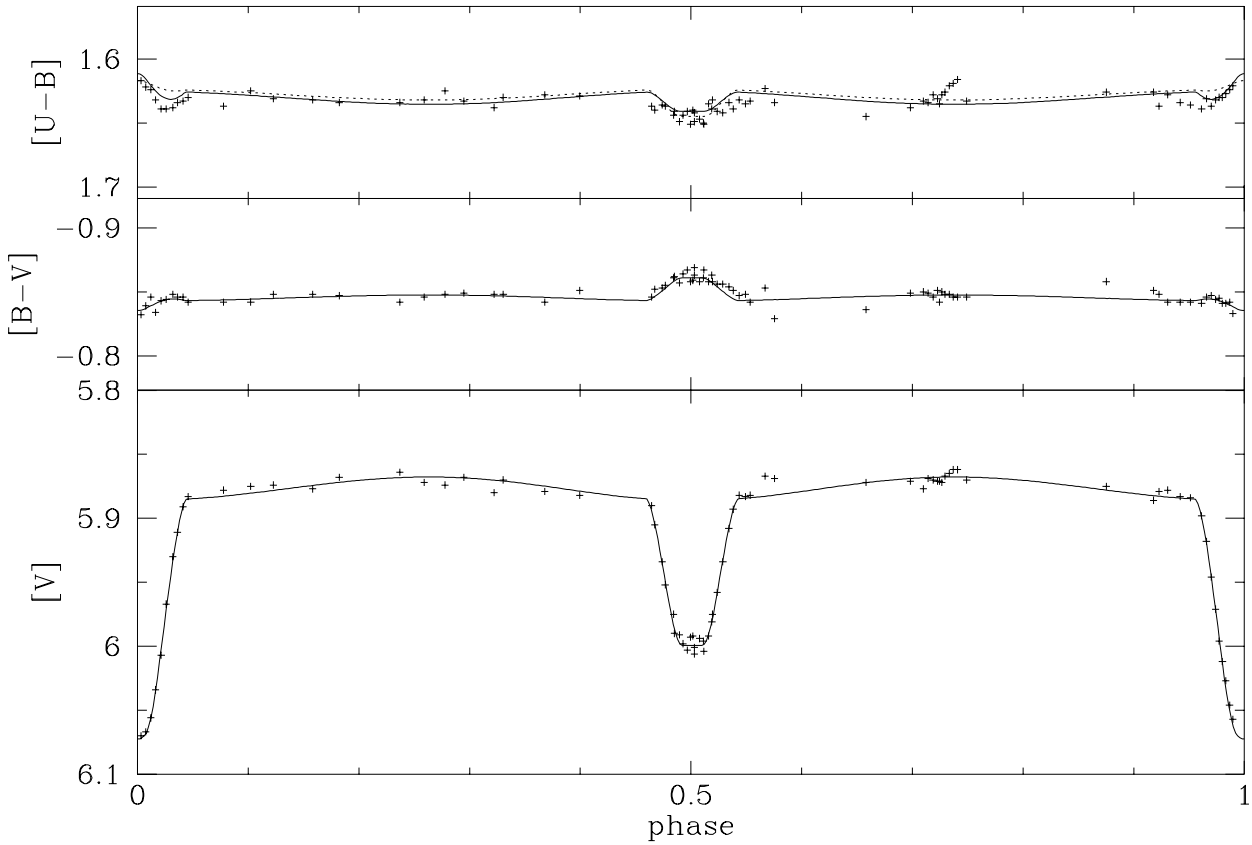

Fig. 8. Lightcurves of HD 184035 in the V magnitude and in the $[U-B]$ and $[B-V]$ indices. The fitted lightcurves are those computed by the WINK code for the adopted parameters of Table 13. For $[U-B]$, the dotted line corresponds to a standard limb-darkening coefficient of the primary in the $[U]$ band, while the continuous line is for $u_1([U])$ = 0.21 (see text).

Table 11. Magnitude and colours of each component of HD 184035. The combined colours of the whole system are given too.

object	m_V	$[U-B]$	$[V-B]$	$[B1-B]$	$[B2-B]$	$[V1-B]$	$[G-B]$	$\Delta(V1-G)_o$	Δm_2
primary (ϕ = 0.5)	5.999	1.645	0.863	0.901	1.477	1.563	2.036	-0.009	-0.007
primary (ϕ = 0.25)	5.980	1.644	0.865	0.901	1.477	1.566	2.039	-0.009	-0.003
secondary	8.399	1.490	0.678	0.981	1.425	1.368	1.782	-0.009	0.001
whole system (ϕ = 0.5)	5.884	1.632	0.846	0.907	1.472	1.545	2.012		
whole system (ϕ = 0.25)	5.869	1.631	0.848	0.907	1.473	1.548	2.015		

efficiently, so the fitted values are fanciful, exceeding one in some instances. Therefore as a first step, we imposed the values interpolated in the tables of Wade & Rucinski (1985) for the relevant temperatures and surface gravities. The maximum ellipticity (i.e. that of the meridian passing through the poles and the system's axis) of the primary is 0.988 and its equatorial ellipticity is 0.994, while the maximum ellipticity of the secondary is 0.998.

The quantities $e\cos\omega$ and $e\sin\omega$ have been fitted, with the result that both seem marginally significant, i.e. close to the 3-sigma level. A non-zero eccentricity would qualitatively agree with the spectroscopic data (see below).

When the adopted geometrical elements are imposed in all seven magnitudes, the result is satisfactory in all passbands but [U]: strangely enough, we have to decrease the limb-darkening of the primary down to u_1 = 0.21 to obtain a good fit of the primary minimum. Equivalently, we obtain a larger radius of the primary in the [U] band if we fix the limb-darkening to its tabulated value. In Fig. 8, we show two theoretical curves for the $[U-B]$ index: the full line is for u_1 = 0.207 and $T_{\rm eff}$ = 7281K which result from a fit where all other parameters have been fixed to their adopted value; the dotted line is for u_1 = 0.514 (value interpolated in the published theoretical tables) and $T_{\rm eff}$ = 7350K. It is quite plain that the latter cannot reproduce well the primary minimum; even the curve corresponding to the small u_1 value is not fully satisfactory. We cannot offer any explanation for this behaviour at present. The number of measurements being relatively small in the primary minimum, it would be useful to make additional ones at these phases.

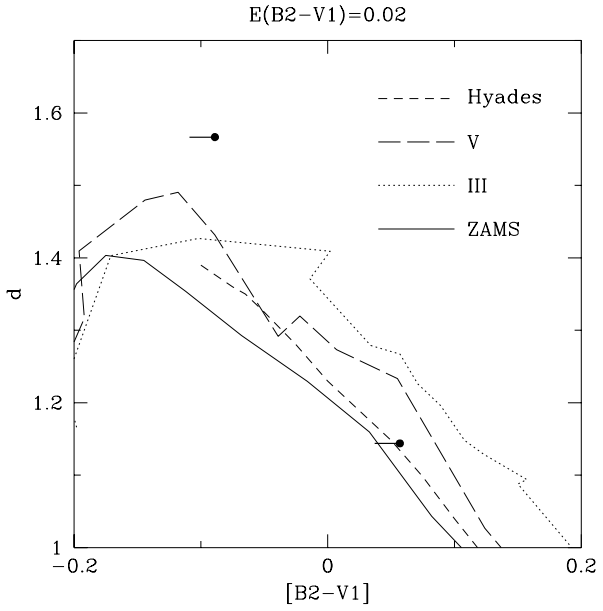

Fig. 9. Position of the components of HD 184035 in a d/B2-V1 photometric diagrams. Symbols are the same as for Fig. 2. The effect of a small colour excess $E(B2-V1) = 0.02$ is shown, although the real reddening is probably negligible.

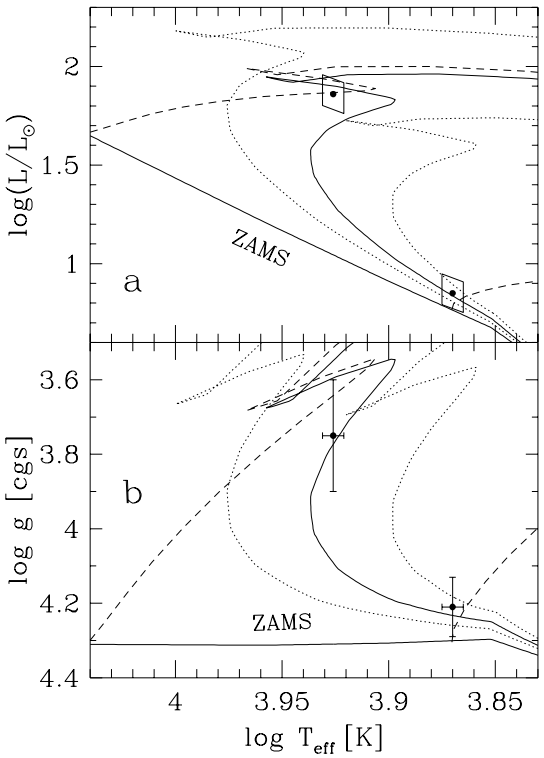

Fig. 10. a HR diagram of the HD 184035 system assuming $M_2 = 1.572\,M_\odot$. The solid lines are the theoretical ZAMS and the isochrone at $\log t = 8.75$ (t in years) from Schaller et al. (1992). The dotted lines are the isochrones at $\log t = 8.6$ and 8.9. The observed location of the components is indicated by the black dots and error boxes. The errors are the amplified ones of Table 15. The dashed lines crossing the isochrones are the evolutionary tracks for $2.59\,M_\odot$ (which is smaller than the M_1 value estimated from the mass function) and $1.572\,M_\odot$. **b** Same as **a**, but for the surface gravity instead of luminosity on the y-axis. The isochrones shown correspond to the metallicity $Z = 0.020$.

Table 12. Physical parameters obtained from the Geneva colour indices for each component of the system HD 184035, using the calibration by Künzli et al. (1997) (abbreviated KNKN97). The effective temperatures obtained using the calibration of Hauck & Künzli (1996) (abbreviated HK96) are given too.

object	calibration	$T_{\rm eff}$ [K]	$\log g$ [cgs]	$[M/H]$ [dex]
primary	KNKN97	8425	3.53	
		±80	±0.11	
secondary	KNKN97	7415	4.30	0.19
		±65	±0.07	±0.08
primary	HK97	8695		
secondary	HK97	7513		

Another striking anomaly is the gradual decrease of the $[U-B]$ index from $\phi = 0.71$ to $\phi = 0.74$. These measurements were made at increasing airmass (from 1.05 to 1.59) in the night of 18–19 July, while most of the standard stars were at low airmass (only "all-sky", not differential measurements were made) so we cannot guarantee that the variation is intrinsic and not due to a biased estimate of the atmospheric extinction in the $[U]$ band. Such a bias might also be responsible for the anomalous limb-darkening value we obtain in the $[U]$ band for the primary.

Finally, considering a third light in the fit results in $L_3 = 0.22 \pm 0.06$ for the $[V]$ band (the result is similar in the $[B]$ band) and $\sigma_{res} = 0.0034$, still with $w_1 = w_2 = 0$. The improvement of σ_{res} is so small that this result is probably not significant. If $w_1 = w_2 = 1$, one obtains a negligible $L_3 = 0.03 \pm 0.06$, but with $\sigma_{res} = 0.050$.

3.2.2. Radial velocities

We have reanalyzed the data published by Buscombe & Morris (1961), using a half-weight for those obtained with the 2-prism Newtonian spectrograph (with respect to those obtained with the 3-prism Cassegrain one). We imposed the orbital period at the 4.6283-days value derived from our photometry, and fitted an orbit both allowing e to be adjusted and with e fixed to zero. The results are shown in Table 14. Leaving the orbital period free would lead to $P = 4.6261 \pm 0.0006$ days, with a significant improvement in the scatter of the residuals (5.2 km s^{-1}), but such a period is too short to be compatible with the photometric one. Our orbital parameters are consistent with those of Buscombe & Morris within the errors, except for ω which is smaller by as much as 3 sigmas.

The standard deviation of the residuals is very large; the eccentricity might be non-zero but is only 71% larger than its uncertainty, so that it cannot be considered as significant. In any case, it is much less so than the (smaller) eccentricity suggested by the lightcurve. Another indication that it is not meaningful

Table 13. WINK10 solution of the 7 lightcurves of HD 184035. In all cases the limb-darkening coefficients have been kept fixed, except for $[U]$ where it has been determined together with $T_{\rm eff2}$ with all other parameters fixed to their adopted values. The adopted parameters are listed in the last column.

parameter	$[U]$	$[B]$	$[V]$	$B1$	$B2$	$V1$	G	Adopted
i (degrees)	83.15	84.44	84.02	84.17	83.91	83.96	83.60	83.94
	±0.43	±0.28	±0.22	±0.29	±0.25	±0.23	±0.23	±0.22
$e\cos\omega$	0.00166	0.00180	0.00212	0.00203	0.00146	0.00188	0.00164	0.00181
	±0.00091	±0.00066	±0.00049	±0.00073	±0.00057	±0.00050	±0.00049	±0.00049
$e\sin\omega$	-0.043	-0.053	-0.0366	-0.038	-0.045	-0.035	-0.030	-0.039
	±0.018	±0.012	±0.0096	±0.013	±0.011	±0.011	±0.011	±0.011
e	0.043	0.053	0.0367	0.038	0.037	0.035	0.030	0.039
	±0.018	±0.012	±0.0096	±0.013	±0.012	±0.011	±0.011	±0.011
ω [°]	-87.8	-88.1	-86.7	-86.9	-87.8	-86.9	-86.9	-87.4
	±1.5	±0.8	±1.2	±1.5	±1.1	±1.3	±1.5	±1.0
r_1/a	0.2120	0.1968	0.2016	0.2006	0.2020	0.2039	0.2055	0.2025
	±0.0022	±0.0018	±0.0010	±0.0020	±0.0017	±0.0020	±0.0017	±0.0010
k	0.4180	0.4026	0.4034	0.4061	0.4121	0.4059	0.4113	0.4063
	±0.0070	±0.0062	±0.0026	±0.0065	±0.0064	±0.0049	±0.0054	±0.0026
r_2/a	0.0886	0.0792	0.08133	0.08146	0.0832	0.0828	0.0845	0.08228
	±0.0018	±0.0014	±0.00066	±0.0015	±0.0015	±0.0013	±0.0013	±0.00066
u_1	0.514	0.623	0.487	0.596	0.601	0.500	0.448	$[U]$: 0.207
u_2	0.638	0.591	0.494	0.579	0.575	0.514	0.434	
$T_{\rm eff\,2}$	7211	7587	7588	7686	7643	7648	7622	$[U]$: 7350
	±35	±9	±7	±36	±35	±36	±40	
σ_{res} (mag)	0.0065	0.0044	0.0037	0.0045	0.0040	0.0038	0.0039	

Table 14. Orbital elements of the HD 184035 system, for e "free" and for e "fixed" respectively. The second line gives the uncertainty on the fitted parameters. Zero uncertainty means that the corresponding parameter was considered as known and was kept constant.

Star name	P	T$_\circ$ HJD	e	V$_\circ$	ω_1	K$_{1,2}$	$f_{1,2}(\mathscr{M})$	a$_1$ sin i	N	(O-C)
	$days$	-2430000		kms^{-1}	°	kms^{-1}		10^6km		kms^{-1}
HD 184035	4.62830	7001.470	0.072	12.3	195	71.6	0.175	4.54	16	7.34
	0.00000	0.026	0.042	2.0	40	3.3	0.024	0.20		
HD 184035	4.62830	6998.968	0.000	13.0	0.0	69.5	0.162	4.42	16	7.93
	0.00000	0.030	0.000	2.1	30	3.1	0.022	0.20		

is the associated value of ω, the longitude of the periastron: it is close to 180°, while $\omega \sim -90$° according to the lightcurve. We may conclude that there might be a slight eccentricity, but more photometric and radial-velocity data are needed to settle the question. High S/N observations should be able to reveal the companion (e.g. through the Na I D lines) in spite of the large luminosity difference and relatively fast rotational velocities; one may expect the lines of the companion to be no deeper than 2%, but this should be enough.

The question whether e is zero or not is an interesting and important one, regarding especially the theories of circularisation (Zahn 1977, 1978, Tassoul & Tassoul 1992): since the primary is evolved, the system's age is well defined, so we have here a possibility to test these theories rather precisely. Alternatively, a non-zero eccentricity might be due to the presence of an as yet undetected third companion.

Physical properties of the HD 184035 system: An interpolation in the evolutionary tracks of Schaller et al. (1992) for Z = 0.020 (using a code kindly made available by Jordi & Figueras, 1994) gives M_2 = 1.572$M_\odot$ and $\log t$ = 7.9 for the secondary, whose colours (hence $T_{\rm eff}$ and $\log g$) may be more reliable than those of the primary because of the lack of tidal distorsion. Using the measured mass function and assuming no error on the secondary's mass, we then obtain M_1 = 3.28 ± 0.28$M_\odot$ (taking at face value the formal error on the mass function is given in Table 14) and the other physical parameters which follow are listed in Table 15. All uncertainties on the masses and radii have been arbitrarily amplified by a factor of two relative to the formal errors of Tables 13 and 14, as for TV Nor. Here the uncertainties (e.g. on the radii) linked with the radial-velocity curve largely dominate over those linked with the lightcurve. The way in which the physical parameters change when M_2 is varied by ±10% is also shown. The projected rotational velocity expected from synchronism is 43.6±4.4 km s^{-1} for the primary, and 17.8 ± 1.8 km s^{-1} for the secondary. The existing $v\sin i$ values, which hold for the primary, are 22% to 38% larger, suggesting that synchronism has not yet taken place. However, the uncertainty on the measured values may be enough to explain the difference.

Table 15. Physical parameters of the components of HD 184035. The errors on the masses and radii have been doubled (with respect to those in Tables 13 and 14) in order to make them more realistic. The numbers between parentheses indicate the result obtained when M_2 is decreased, respectively increased by 10%.

	Primary (M_2 -10%, +10%)	Secondary (M_2 -10%, +10%)
$M/M_\odot$	3.28 ± 0.56	1.572
	(2.73, 3.87)	(1.415, 1.729)
$R/R_\odot$	4.00 ± 0.36	1.63 ± 0.15
	(3.79, 4.19)	(1.54, 1.70)
$\log g$ [cgs]	3.75 ± 0.15	4.21 ± 0.08
	(3.72, 3.78)	(4.21, 4.21)
$v \sin i$ [km s^{-1}]	60 ± 9 (or 53)	
$\log T_{\rm eff}$ [K]	3.926 ± 0.005	3.870 ± 0.005
$\log L/L_\odot$	1.86 ± 0.11	0.85 ± 0.10
	(1.81, 1.90)	(0.81, 0.90)
M_{bol}	0.10 ± 0.25	2.61 ± 0.25
	(0.22, 0.00)	(2.73, 2.51)
$B.C.$	-0.16	-0.10
M_v	0.26 ± 0.25	2.71 ± 0.25
	(0.38, 0.16)	(2.83, 2.61)
Distance [pc]	138 ± 16	
	(132, 147)	(130, 144)

The position of both components in the HR diagram is shown in Fig. 10, together with the ZAMS and with the isochrone at $\log t$ = 8.75 which best fits them. The evolved state of the primary, suggested above by the colour indices, is entirely confirmed here. The isochrone, based on Schaller et al. (1992) corresponds to a metallicity Z = 0.020. There is a problem with the mass of the primary, since the evolutionary track corresponding to 3.28 $M_\odot$ (the mass estimated from the mass function and an assumed secondary's mass) is much higher than the observed point. The evolutionary track represented in Fig. 10 was interpolated for $M = 2.59 M_\odot$, which would correspond to a mass function $f(m) = 0.22 M_\odot$, i.e. 2.64 σ larger than the observed one. Although unexpectedly large, such a discrepancy remains statistically possible; a 0.25 phase gap around the minimum in the radial-velocity curve may be responsible for a biased value of the mass function. Clearly, this system would deserve to be measured again with both spectroscopy and photometry, since the dissimilarity of its components makes it interesting for a test of evolution models.

3.3. HD 185257 (HD 7464, V4090 Sgr)

The V lightcurve of this system has been studied by Giuricin et al. (1984) by means of the WINK code. They concluded that both components are on the main sequence, with spectral types A5m and G, and stressed the interest of having here two very dissimilar components. We propose below a more detailed analysis involving not only one lightcurve, but also the six others measured simultaneously in the Geneva photometric system, which will give a better idea of the uncertainties on the geometrical parameters. Furthermore, radial velocities found in the literature are used to constrain the mass ratio and obtain an independant estimate of the eccentricity and longitude of the periastron.

3.3.1. Photometry

Using the same period-search method as before, we obtain a period which differs very slightly from that of Waelkens & Rufener (1983):

$$HJD(Min.I) = \begin{array}{l} 2441174.7319 + 11.41510E \\ \pm 0.0010 \quad \pm 0.00012 \end{array} \qquad (6)$$

There are 445 photometric measurements in each passband, most of which, unfortunately, outside the eclipses. This situation is due to the fact that this star had been used as a photometric standard until its eclipses were discovered. A relatively large fraction of the data (144) have a low or moderate photometric weight $Q \leq 2$, so the analysis was restricted to the 301 good-quality data (Q = 3 and 4). Fig. 11 shows the light and colour curves. The depth of both minima is very small, but one can clearly see that the secondary minimum does not fall right at phase 0.5, so the orbit is eccentric.

The scatter of the residuals is slightly larger than expected for such a bright star (0.0056 mag. instead of $\sim$ 0.004 mag.), suggesting a possible δ Scuti-type variation of the primary. However, a period search on the visual, out-of-eclipse magnitudes in the frequency range 15-28 cycles/day (suggested by the period-gravity relation of Fernie 1995) remained unsuccessful. Indeed, only marginal Am stars may pulsate, so a positive result would have been rather surprising for an Am strong enough to be detected by photometry alone.

Effective temperatures of the components: We have compared the effective temperatures proposed by Giuricin et al. (1984), i.e. $T_{\rm eff1}$ = 8100K and $T_{\rm eff2}$ = 5770K, with the values obtained from the Geneva colours assuming a total eclipse in the secondary minimum. Using the calibration of Künzli et al. (1997), we find $T_{\rm eff1}$ = 7649 $\pm$ 70K, $\log g_1$ = 4.30 $\pm$ 0.07 and $[M/H]_1$ = 0.36 $\pm$ 0.07 for the primary. But the colours of the secondary, deduced from those of the whole system and of the primary, are too far from normal (the d parameter especially, is too small) to allow the use of this calibration. Using only the $B2-V1$ index (0.369) and its calibration by Hauck & Künzli (1996) leads to $T_{\rm eff2}$ = 5812K, which is compatible with the value (5770) given by Giuricin et al. (1984). Our estimate of the effective temperature for the primary can be biased only slightly by the assumption of a total eclipse, because the much bolder assumption of a negligible brightness of the secondary (i.e. using the colours of the whole system at quadratures) leads to a temperature which is only 100–140 K lower. Our $T_{\rm eff1}$ determination may be underestimated by at most 50 K, so we adopted the values $T_{\rm eff1}$ = 7700 K and $T_{\rm eff2}$ = 5800 K for the interpolation of the limb-darkening coefficients.

Preliminary estimates of the components' radii were used, as well as photometric estimates of the masses to obtain the surface gravities $\log g_1$ = 4.07 and $\log g_2$ = 4.42 which are also necessary to define the limb-darkening.

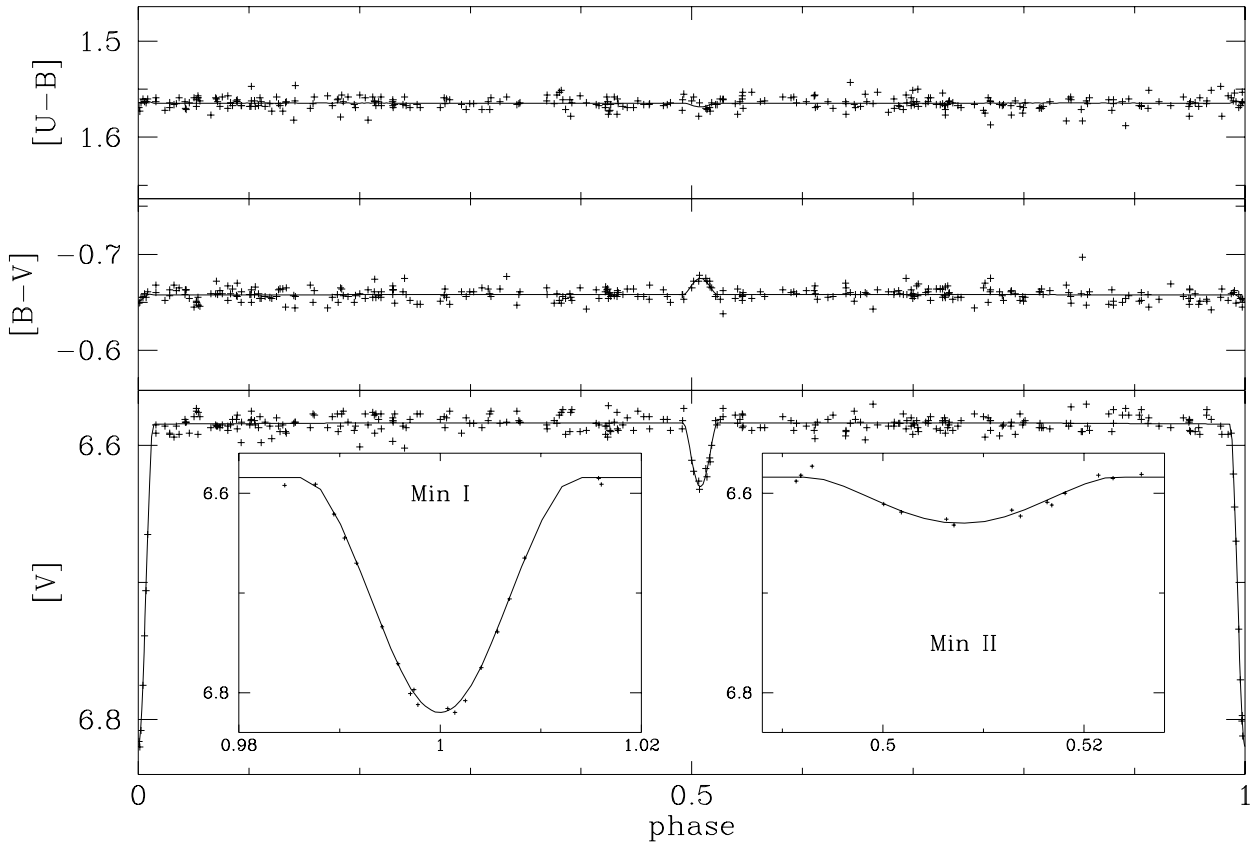

Fig. 11. Lightcurves of HD 185257 in the V magnitude and in the $[U-B]$ and $[B-V]$ indices. The fitted lightcurves are those computed by the EBOP code for the adopted parameters of Table 16.

Determination of the photometric parameters: For this star, we have used only the EBOP code since the period is long and the system is very wide. The limb-darkening coefficients have been interpolated in the tables of Wade & Rucinski (1985). Since the eclipses are probably not total, the convergence is more difficult than in the two other cases. Furthermore, the orbit is not circular but slightly elliptic. Fixing all elements but $e\cos\omega$, $\Delta\theta$ (the phase correction of the primary minimum) and $SFACT$ (the magnitude normalisation of the lightcurve), one obtains consistently $e\cos\omega = 0.0124$ with a 10 % probable error for all seven lightcurves. This parameter being fixed, we tried to obtain a convergence for all other geometric parameters (r_1, k, i and $e\sin\omega$) and for J_s, (the ratio of central surface brightnesses) and succeeded for all colours but $B1$. One obtains $e\sin\omega \sim 0.10$ with a probable error of about 100%; in spite of such a large error, $e\sin\omega$ is always positive and the 6 estimates are coherent. From the 6 lightcurves alone, one finds $e = 0.102 \pm 0.025$ and $\omega \approx 83 \pm 1.6^{\circ}$, where the uncertainties are the rms standard deviations of the 6 values obtained from the individual lightcurves. From the radial-velocity curve, one has $e = 0.109 \pm 0.030$ and $\omega = 99 \pm 14^{\circ}$ (see next paragraph). It is encouraging that both determinations of e and ω agree so well, although ω derived from radial velocities is clearly overestimated: according to the lightcurves, its true value must be smaller than 90 degrees. To obtain the inclination, radii and surface brightness ratios, the values $e = 0.10$ and $\omega = 83^{\circ}$ were adopted and fixed. The results are shown in Table 16. There is clearly a very strong correlation between the inclination i and the ratio of radii k, so that both values are rather uncertain.

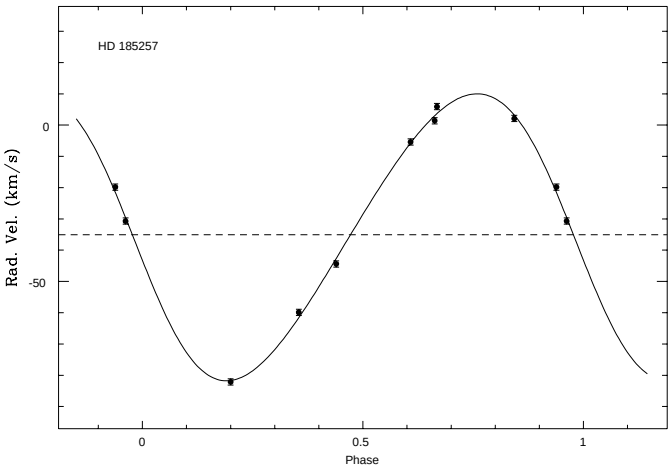

Fig. 12. Radial velocity curve of HD 185257, based on the measurements of Catchpole et al. (1982) and of Nordström & Andersen (1985).

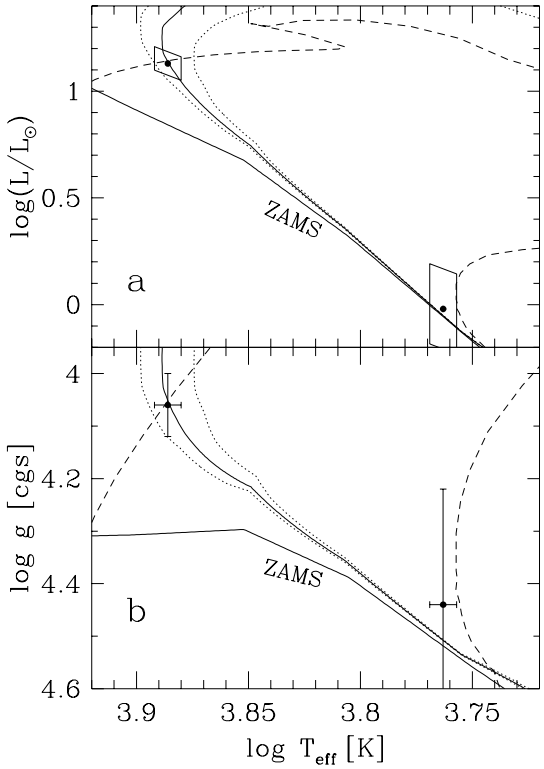

Fig. 13. a HR diagram of the HD 185257 system, with the isochrone at $\log t$ = 8.94 and assuming M_1 = 1.81 $M_\odot$. The dotted lines are the isochrones at $\log t$ = 8.9 and 9.0, the broken lines are the evolutionary tracks for M_1 = 1.81 $M_\odot$ and M_2 = 0.95 $M_\odot$. Same indications as in Fig. 7. **b** Same as **a**, but for the surface gravity instead of luminosity on the y-axis. The errors are the amplified ones of Table 18.

Numerical experiments on 10 synthetic $[V]$ lightcurves sampled at the observed phases and affected by a random noise have been performed to test the reliability of the results. Eight out of the ten simulated data sets gave reasonable results (i, r_1/a, k, J_2/J_1 and $SFACT$ were converged simultaneously), while the other two gave wild values, especially for k, but interestingly the formal errors were much larger (up to ten times) in these cases. Discarding the two unreliable fits, the external rms scatter of the fitted parameters (computed from the eight remaining curves) was found smaller than the formal error in all cases but r_1/a, for which σ_{ext} = 0.0020 while σ_{formal} = 0.0011. We also tested - this time on the real, observed data - the range of k values compatible with the $[V]$ lightcurve: imposing k = 0.40 worsens the fit very significantly, Min II becoming a *total* eclipse, and the bottom of Min I is not well reproduced yet with k = 0.42. Therefore, the *lower limit* of k is very well constrained. On the other hand, k may increase to arbitrarily large values (i.e. 1.0 and even beyond) without degrading much the fit; if it is released and the code tries to find its value, convergence is achieved as long as it starts from $k \leq 0.66$, while the code collapses with a "garbage elements" message as soon as the initial $k \geq 0.68$. Here, the upper limit of k is better obtained from astrophysical arguments than from the lightcurve proper.

Table 18. Physical parameters of the components of HD 185257. The errors on the masses and radii have been doubled (with respect to those in Table 16 and 17) in order to make them more realistic. The numbers between parentheses indicate the result obtained when M_1 is decreased, respectively increased by 10%.

	Primary (M_1 -10%, +10%)	Secondary (M_1 -10%, +10%)
$M/M_\odot$	1.81	0.95 ± 0.08
	(1.63, 1.99)	(0.90, 1.00)
$R/R_\odot$	2.07 ± 0.13	0.97 ± 0.21
	(2.02, 2.13)	(0.94, 1.00)
$\log g$ [cgs]	4.06 ± 0.06	4.44 ± 0.22
	(4.04, 4.08)	(4.44, 4.44)
$\log T_{\rm eff}$ [K]	3.886 ± 0.006	3.763 ± 0.006
$\log L/L_\odot$	1.13 ± 0.08	-0.02 ± 0.21
	(1.11, 1.16)	(-0.04, 0.00)
M_{bol}	1.92 ± 0.20	4.80 ± 0.53
	(1.98, 1.86)	(4.86, 4.74)
$B.C.$	-0.11	-0.21
M_v	2.03 ± 0.20	5.01 ± 0.53
	(2.09, 1.97)	(5.07, 4.95)
Distance [pc]	85 ± 10	
	(81, 86)	(87, 92)

3.3.2. Radial velocities

In addition to the six radial velocities of Catchpole et al. (1982)[1], there are three values published by Nordström & Andersen (1985). Nine values are just enough to attempt an orbit determination, whose result is shown in Table 17 and Fig. 12. The period was fixed to its photometric value. Both e and ω are compatible with those estimated from the lightcurves, in spite of their large uncertainties. The lightcurve gives a better estimate of ω through the quantity $e \cos\omega$, as discussed above.

Physical properties of the HD 185257 system: An interpolation in the evolutionary tracks gives M_1 = 1.81$M_\odot$ and $\log t$ = 8.94 for the primary. Using the measured mass function and assuming no error on the primary's mass, we then obtain M_2 = 0.95 $\pm$ 0.04$M_\odot$ and the other physical parameters which follow are listed in Table 18; here the errors on the masses and radii have been arbitrarily doubled, as before. The way in which these parameters change when M_1 is varied by $\pm$10% is also shown. The position of both components in the HR diagram is shown in Fig. 13, together with the isochrone at $\log t$ = 8.94 which best fits them. The primary appears slightly but significantly evolved. Interestingly, the Hipparcos parallax of this system is π = 11.84 $\pm$ 0.97 mas, corresponding to a distance of 84.5 $\pm$ 7.0 pc: this matches perfectly our completely independant estimate!

4. Discussion

We have examined three eclipsing binaries possibly containing a CP star according to their spectral classification or low rotational

[1] There is a typographical error in their paper: the epoch of their 5th measurement of HD 185257 must read JD 37518.4 instead of 37158.4

Table 16. EBOP16 solution of the 7 lightcurves of HD 185257. In all cases the limb-darkening coefficients have been kept fixed. $e\cos\omega$ and $e\sin\omega$ were both converged in a first series of iterations, then they were kept fixed at 0.01219 and 0.09926 respectively (see text), which corresponds to e = 0.10 and ω = 83°. The adopted geometric parameters are listed in the last column.

parameter	$[U]$	$[B]$	$[V]$	$B1$	$B2$	$V1$	G	Adopted
i (degrees)	87.21	87.05	87.26	87.2	86.8	86.6	87.33	87.19
	±0.86	±0.97	±0.48		±1.3	±1.4	±0.63	±0.48
r_1/a	0.0685	0.0696	0.0698	0.0696	0.0697	0.0694	0.0694	0.0695
	±0.0014	±0.0012	±0.0011	±0.0012	±0.0026	±0.0063	±0.0016	±0.0011
k	0.477	0.49	0.463	0.4683	0.52	0.56	0.459	0.468
	±0.096	±0.12	±0.048	±0.0086	±0.20	±0.29	±0.061	±0.048
r_2/a	0.0327	0.0339	0.0323	0.03259	0.036	0.039	0.0319	0.0325
	±0.0066	±0.0084	±0.0034	±0.00083	±0.014	±0.020	±0.0043	±0.0034
u_1	0.621	0.551	0.471	0.568	0.533	0.476	0.451	
u_2	0.864	0.779	0.622	0.807	0.736	0.631	0.593	
J_2/J_1	0.198	0.172	0.272	0.143	0.221	0.31	0.293	
	±0.041	±0.043	±0.030	±0.021	±0.078	±0.13	±0.041	
σ_{res} (mag)	0.0083	0.0064	0.0056	0.0074	0.0072	0.0067	0.0081	

Table 17. Orbital elements of the HD 185257 system. The second line gives the uncertainty on the fitted parameters. Zero uncertainty means that the corresponding parameter was considered as known and was kept constant.

Star name	P $days$	T$_\circ$ HJD -2440000	e	V$_\circ$ kms^{-1}	ω_1 °	K$_{1,2}$ kms^{-1}	$f_{1,2}(\mathscr{M})$	a$_1$ sin i $10^6 km$	N	(O-C) kms^{-1}
HD 185257	11.4151	2658.98	0.109	-35.09	99.2	45.88	0.1125	7.15	9	2.19
	0.0000	0.43	0.029	0.81	13.9	1.39	0.0103	0.20		

velocity. Among them, only one, HD 185257, has a confirmed CP primary of the Am type. TV Nor, although classified EuCrSr, very probably has a normal secondary, while there is only very marginal evidence that the primary may be a mild Ap: Na seems slightly overabundant and the $\Delta(V1-G)$ has a small positive value; furthermore, no out-of-eclipse variation is apparent, so that there is no intrinsic variation typical of magnetic Ap stars. One might wonder whether the primary of TV Nor is an HgMn-type Ap, since these stars do have a slightly larger $\Delta(V1-G)$ than normal stars. Only the measurement of Hg and Mn lines will settle the question (Si, Cr and Sr lines should be examined too), and such a test would be worth the effort.

As for HD 184035, where $v\sin i \sim 60$ km s^{-1} (Levato 1975) or 53 km s^{-1} (Hoffleit & Jaschek 1982) for the primary, no clear indication of any kind of chemical peculiarity can be found in the photometric data. Neither the shape of the lightcurve nor the peculiarity parameters betray the CP nature one could suspect from the relatively low equatorial velocity. Of course, more subtle chemical anomalies might be present which would have no effect on the photometry but could be seen on high-resolution spectra. This system is quite interesting in this respect, to test the idea of Abt & Morrell (1995) that $v\sin i$ is the only parameter that distinguishes normal and pronounced or mild CP stars. However, the tidal distorsion and corresponding variation of the temperature on the surface of the star would have to be taken into account in any detailed abundance analysis of the primary.

Another interest presented by these three systems is the synchronism, or lack thereof, between the spin and orbital periods. It seems that syncronism is nearly but not completely achieved in the case of TV Nor, and that it has not yet taken place in the case of HD 184035 - even for the evolved primary - if one takes the published $v\sin i$ at face value. Indeed, the expected $v\sin i$ of the primary of HD 184035 is only 40 km s^{-1} in the case of synchronism. This may appear surprising at first sight, because of the shorter period of HD 184035: the effective temperatures of the components are very similar for HD 184035 and TV Nor; on the other hand, the primary of HD 184035 is significantly more massive than that of TV Nor and might have rotated faster in the past. No $v\sin i$ value has been published to date for HD 185257, but according to Nordström & Andersen (1985), it must lie between 50 and 100 km s^{-1}, so that synchronism has surely not been reached yet, at least for the primary. This is not unexpected, in view of the long period. It would be interesting to know the equatorial velocity of the secondary, which has a relatively thick outer convection zone (contrary to the primary) hence a different way to dissipate the tidal force, besides the magnetic braking through stellar wind. More spectroscopic data on both HD 184035 and HD 185257 would be extremely welcome in this respect, and also to obtain the radial-velocity curves of both companions. It would even be worthwhile to re-observe TV Nor at very high resolution ($R \geq 100\,000$) to obtain more accurate equatorial velocities.

Acknowledgements. We are indebted to Dr. P.B. Etzel and to the regretted Z. Kviz for having transmitted to us the EBOP code and Wood's WINK code. The help of Dr. B. Helt in getting in touch with the WINK program is gratefully acknowledged. The observations, to which Dr. M. Burnet largely contributed, were reduced by Mr. C. Richard. We thank Dr. R.M. Catchpole for having fixed a typing error in his published

radial velocities, and Dr. T. Lanz for having provided the SYNSPEC code. We also thank Dr. R.L. Kurucz for his model atmospheres revised in the summer of 1995, and Mr. F. Betrix for his help in using the SYNSPEC code. The program for building the isochrones from evolutionary tracks has been kindly provided by Dr. G. Meynet. This research has made use of the Simbad database, operated at CDS, Strasbourg, France. It has been supported in part by the Swiss National Science Foundation.

References

Abt H.A., Morrell N.I., 1995, ApJS 99, 135
Andersen J., 1991, A&AR 3, 91
Andersen J., Nordström B., 1977, A&AS 29, 309
Baranne A., Mayor M., Poncet J.L., 1979, Vistas in Astron. 23, 279
Burki G., Cramer N., Mermilliod J.-C., 1993, private communication
Burnet M., Rufener F., 1979, A&A 74, 54
Buscombe W., Morris P.M., 1961, MNRAS 123, 181
Catchpole R.M., Evans D.S., Jones D.H.P., King D.L., Wallis R.E., 1982, Royal Greenwich Obs. Bull. 188, 5
Clausen J.V., Giménez A., van Houten C.J., 1995, A&AS 109, 425
Cramer N., 1994, thesis No. 2692, Geneva University, p. 46
Etzel P.B., 1980, EBOP user's guide (3rd edition), UCLA
Etzel P.B., 1989, private communication to Z. Kviz
Fernie J.D., 1995, AJ 110, 2361
Fuhr J.R., Martin C.A., Wiese W.L., 1988, J. Phys. Chem. Ref. Data 17, Suppl. No 4
Gaspani A., 1984, IBVS 2552
Gerbaldi M., Floquet M., Hauck B., 1985, A&A 146, 341
Giuricin G., Mardirossian F., Mezetti M., 1984, A&A 135, 194
Hauck B., 1973, in: Problems of Calibration of Absolute Magnitudes and Temperature of Stars, IAU Symp. No. 54, eds. B. Hauck and B.E. Westerlund, Reidel, Dordrecht, p. 117
Hauck B., 1974, A&A 32, 447
Hauck B., 1994, in: The MK process at 50 years: a powerful tool for astrophysical insight, A workshop of the Vatican Observatory, eds. R.O. Gray and R.F. Garrison, ASP Conf. Series Vol. 60, p. 157
Hauck B., Curchod A., 1980, A&A 92, 289
Hauck B., Jaschek C., Jaschek M, Andrillat Y., 1991, A&A 252, 260
Hauck B., Künzli M., 1996, Baltic Astronomy 5, 303
Hauck B., North P., 1982, A&A 114, 23
Hertzsprung E., 1937, Bull. Astr. Netherl. 8, 168
Hoffleit D., Jaschek C., 1982, The Bright Star Catalogue, Fourth revised edition, Yale University Observatory
Houk N., 1978, University of Michigan Catalogue of two-dimensional Spectral Types for the HD Stars, Vol. 2, University of Michigan, Ann Arbor
Houk N., 1982, University of Michigan Catalogue of two-dimensional Spectral Types for the HD Stars, Vol. 3, University of Michigan, Ann Arbor
Houk N., Cowley, A., 1975, University of Michigan Catalogue of two-dimensional Spectral Types for the HD Stars, Vol. 1, University of Michigan, Ann Arbor
Johansen K.T., Nordström B., 1995, IBVS 4135
Jordi C., Figueras F., 1994, private communication
Kruytbosch W.E., 1930, Bull. Astr. Netherl. 6, 15
Künzli M., North P., Kurucz R.L., Nicolet B., 1997, A&AS, 122, 51
Kurucz R.L., 1989, Magnetic tape with iron-peak elements line list ("gfiron"), private communication
Kurucz R.L., 1995, private communication
Levato H., 1975, A&AS 19, 91
Lucke P.B., 1978, A&A 64, 367
Moore C.E., Minnaert M.G.J., Houtgast J., 1966, The solar spectrum 2935Å to 8770Å, NBS Monograph 61
Nordström B., Andersen J., 1985, A&AS 61, 53
Nordström B., Johansen K.T., 1994, A&A 282, 787
North P., 1984, thesis No. 2117, Geneva University, p. 96
North P., 1994, in: The 25th workshop and meeting of European working group on CP stars, eds. I. Jankovics and I.J. Vincze, Gothard Astrophysical Observatory of Eötvös University, Szombathely, Hungary, p. 3
North P., Burnet M., 1994, IBVS 4124
North P., Berthet S., Lanz T., 1994, A&A 281, 775
North P., Richard C., 1995, IBVS 4147
Piskunov N.E., Kupka F., Ryabchikova T.A., Weiss W.W., Jeffery C.S., 1995, A&AS 112, 525
Renson P., 1978, A&A 63, 125
Renson P., 1990, IBVS 3452
Schaller G., Schaerer D., Meynet G., Maeder A. 1992, A&AS 96, 269
Tassoul J.-L., Tassoul M., 1992, ApJ 395, 259
Vidal C.R., Cooper J., Smith E.W., 1973, ApJS 25, 37
Vincent A., Piskunov N.E., Tuominen I., 1993, A&A 278, 523
van't Veer-Menneret C., Coupry M.F., Burkhart C., 1985, A&A 146, 139
Wade G.A., North P., Mathys G., Hubrig S., 1996, A&A 314, 491
Wade R.A., Rucinski S.M., 1985, A&AS 60, 471
Waelkens C., Rufener F., 1983, A&AS 52, 13
Whittet D.C.B., 1974, MNRAS 168, 371
Wood D.B., 1972, A Computer Program for Modeling Non-Spherical Eclipsing Binary Star Systems, Publ. of the Goddard Space Flight Center X-110-72-473
Wu Chi-Chao, Gilra D.P., van Duinen R.J., 1980, ApJ 241, 173
Zahn J.-P., 1977, A&A 57, 383
Zahn J.-P., 1978, A&A 67, 162

This article was processed by the author using Springer-Verlag LaTeX A&A style file *L-AA* version 3.